

THE PERFORMANCE OF SWEEPNIK I

R.D. Baker, D.J.M. Davies and G.S.B. Street,
Cavendish Laboratory,
Cambridge, England.

1. Introduction

Sweepnik I was never intended to be a model for routine measuring of events. Nevertheless it has afforded valuable guide lines for the design of its successor Sweepnik II. Preliminary results were reported⁽¹⁾ in November 1968 and since this time further experience has been gained, both in the measurement of conventional events and in the exploitation of the machine in a novel context. In this report we describe some of these results and point out related improvements in Sweepnik II.

2. Measurement of conventional events

In figure (1) (taken from Ref. (1)) we show a comparison of Sweepnik's accuracy with that of one of our conventional film-plane digitizers (a CLARA).

We show the helix fit errors for the same sample of events of the type $pp \rightarrow pp\pi^+\pi^-$

at 16 Gev/c taken in the CERN 2m HBC, when measured on each machine. The sample is restricted to $p_p > 2\text{Gev}/c$ and $p_\pi > 0.4 \text{ Gev}/c$, so that Coulomb errors \ll measurement errors. Sweepnik is better by a factor of 2-3, its errors peaking at 2-3 μm . 95% of these events went on to give good 4C fits.

During the past 12 months some 1600 events (3 prongs from 8 Gev/c np collisions) in the 1.5 m BNHBC have been measured with a view to continuing our assessment of Sweepnik's performance but also to develop a new form of automatic event measurement (akin to minimum guidance). This facility works as follows. The probe is positioned on the vertex with the aid of a closed-circuit TV system, which shows the film under a great magnification at the probe's current position. (Fig. 2a shows a 3-prong event with the TV reference cross centered on it). On

request, the computer takes over from the operator digitizing the angles of the various tracks originating at the vertex. (Fig. 2b shows the analogue signal obtained and the squared pulses used by the computer). Some checks are carried out to ensure that such pulses do belong to tracks coming from the vertex.

Each track is then followed by the machine.

Of the 1600 3-prong events, 75% passed geometry on the first try; 17% failed due to track inversion and 7% due to vertex inversion. Software changes have already been made to avoid the last source of error. These move the probe to selected "good" events on views 2 and 3. Track inversion could be avoided in most cases with simple checks.

In figure 3 we show the helix fit errors for 4800 tracks from these events. The mean error of 5 μm s is somewhat higher than the 2-3 μm s obtained on the specially selected set of pp events at 16 Gev/c. However it is an overall figure for all momenta and obtained from the 1.50 m BNHBC for which the geometrical constants are known to be imperfect.

CLARA measurements indicate that about 160 3C fits should have been obtained on this batch of events and 145 were obtained. In figures 4 and 5 we show the χ^2 distribution and missing-mass distribution for the fitted events.

3. Use of θ/s plot

Because of Sweepnik's principle of operation, its natural track following coordinates are θ , the angle the track segment makes w.r.t. an absolute zero on the film plane, and s , the number of 1 mm. steps taken down the track. Because curvature is $d\theta/ds$, a straight line plot of these parameters results from a constant curvature track.

An oscilloscope display of θ vs s for each measured track is put out by the on-line PDP7 and this has proved very useful for detecting certain departures of a real track from constant curvature. For the operator's convenience a linear

rise in angle is first subtracted so that a roughly horizontal line would result from a track of constant curvature and direction. Figure 6 shows some typical cases obtained in practice, of (i) a 16 GeV/c proton track with only random fluctuations about a constant $d\theta/ds$; (ii) a low momentum track with large ionisation loss; and (iii) where the probe has been derailed onto the wrong track, enabling the operator to intervene.

A number of important uses of these on-line θ/s plots are indicated;

- i) For segmenting long tracks obtained in future large chambers between significant Coulomb scatters. An angle change of as little as $\frac{1}{2}^\circ$ can be detected as a discontinuity on the θ/s plot, since our empirical RMS angle error is $\sim \frac{1}{8}^\circ$ (see below and Fig. 8).
- ii) For detecting charged particle decays (e.g. of Σ^+) which are often very difficult to detect at the scanning stage, especially so at high energies.
- iii) For detecting radiation losses which, unlike the above, involve negligible angle change but a change in curvature, giving rise to a change in slope on the θ/s plot, without any step on this plot. Figure 7 shows as an example a θ/s plot from a 1 GeV/c electron undergoing a bremsstrahlung so that it loses 53% of its energy.

As an example of the use of (iii) we cite our results from a recent investigation of electron bremsstrahlung based on 40,000 tracks taken in the 1.50m BNHEC. The technique at first adopted was for the operator simply to inspect each θ/s plot and look for a change in slope, indicating an energy loss. Later on a much more efficient technique was to allow the PDP7 to do this in the following way.

The PDP7 routine that decides the position of a discontinuity (ie. step and/or slope-change on the θ/s plot) on a track works by starting near one end of a track, and finding the least squares fit to 2, 3, ...N points. It then

starts from the other end and repeats the process so that fits have been carried out on all pairs of segments into which a given point would divide the θ/s string. The position of least total error is the "best" position of the discontinuity.

Fits to 2..N points on the θ/s plot are carried out by an algorithm relating the fit parameters to N+1 points to that for N. For a slope β_N and error (sum of squares) S_N , we obtain from the conditions

$$\frac{\partial}{\partial \alpha} \sum_1^N (\theta_i - \alpha - i\beta)^2 = \frac{\partial}{\partial \beta} \sum_1^N (\theta_i - \alpha - i\beta)^2 = 0$$

where the θ_i are the angles and $\beta_N = U_N/V_N$ with

$$U_{N+1} = U_N + N\theta_{N+1} - \sum_1^N \theta_i$$

$$V_{N+1} = V_N + \sum_1^N i$$

from which β_{N+1} may be calculated. U_2 is started off as $\theta_2 - \theta_1$, V_2 as 1.

S_n is recalculated each time:

$$S_n = \sum_1^N \theta_i^2 - \left[\left\{ (2N+1) \sum_1^N \theta_i - 3 \sum_1^N i\theta_i \right\} \sum_1^N \theta_i - \beta_N \sum_1^N i\theta_i \right] / \sum_1^{N-1} i$$

At each step the sums

$$\sum_1^N \theta_i, \quad \sum_1^N i\theta_i, \quad \sum_1^N \theta_i^2, \quad \sum_1^N i$$

are updated.

Double length routines are used throughout; the results agree with those obtained on a large (Atlas 2) computer for the same data.

The routine takes ~ 0.2 sec./track, and occupies ~ 550 words ($\sim 0.5k$). It computes the momenta and errors, and lengths of the 2 track segments, and puts out a 'scope display indicating the discontinuity position, for operator intervention. There is now also a significance test, which classifies tracks as having no discontinuity if the total fitted error, normalised to a χ^2 , is within the 5% confidence limit, and if the ratio of the momenta on the 2 "best" segments is $>.9$.

This simple procedure can detect bremsstrahlung losses. The size below which a loss cannot be established seems from more sophisticated fits to be $\rho_2/\rho_1 \sim 0.90$ when ρ_1 and ρ_2 are the curvatures before and after the loss. Position is believed accurate to 1 step (1 mm on film), but this is difficult to verify as small losses cannot be detected by any other method! Errors on the momenta are $\sim 2\%$ for a 1 GeV/c track of length about 1 m. The R.M.S. error in angle measurement is 1.3 counts, i.e. 0.12° , which leads to a position error of 2.0μ per point. Figure 8 shows our experimental error distribution from 4260 tracks which lead to this R.M.S. error of 1.3 counts; the tail is due to the particle slowing down i.e. Coulomb and small bremsstrahlung losses.

In fact, the parameter θ and one initial coordinate (s_0) on the track specifies the complete set of measured points (the step length being a constant 1 mm or so) and there are no accumulative errors. The θ versus constant-increment-in-s representation has 2 distinct advantages over coordinates in searching for deviations from constant curvature, namely;

- 1) Ease of fitting a straight line to equally spaced points; (our PDP7 needs 0.2 s)
- 2) Its independence of rotation in the film plane (initial θ_0 specifies complete direction).
- 3) If necessary (for off-line storage and processing) the information can be stored in a very condensed form (e.g. by specifying θ_0 , $\frac{\partial\theta}{\partial s}$ and the individual small deviations from this straight line. This would allow more sophisticated measurement in a bigger computer e.g. a parabolic fit could be used to take account of ionization loss (2% effect) instead of the straight line fit mentioned above. One could even use fit functions such as $\log \{e^{\alpha(x-x_0)} + 1\} + \beta x$ and so fit best segments directly.

4. Developments in progress

i) Point mode

Although Sweepnik II is now capable of point measurements by the closed-circuit T.V. system, it is intended to develop software capable of using the hardware point-mode facility. This would then enable the machine to find identifiable points without operator intervention. Furthermore, using the experience already gained in detecting discontinuities in the θ/s plot, the machine should automatically detect small-angle scatters on tracks and hence know where to look for a possible stub.

ii) New Logic

New hardware has been designed to detect track pulses at the optimum level for discrimination thus removing this burden from the computer. When the PDP 15 replaces the '7', the speed of the controlling logic will be increased to enable us to further double the speed of track following; it was 5cm/sec on Sweepnik I and is 7.5 cm/sec on Sweepnik II at present, so we expect 15cm/sec. Also, the interface will be capable of handling more than one track measurement per revolution of the probe.

iii) Implications for B.E.B.C.

The first pictures from the BEBC model chamber have proved no problem to Sweepnik I's track detection ability. In Figures 9a, b we see two traces before and after filtering obtained from a picture of 2 closely spaced tracks. We should stress that any noise is film grain and not generated by the system. A criticism that has been raised is that Sweepnik's line image will not be fine enough for the narrow tracks expected. In fact, Sweepnik II has a line width of approximately 12 μm , maintained over the whole film plane by a dynamically

focussed lens. Even narrower tracks are no problem, since, with the excellent signal-to-noise ratio, some loss of pulse height is no embarrassment.

Operator intervention will probably prove a valuable asset in the measurement of film obtained with unconventional optics (e.g. fish eye). We have already mentioned the possible need for segmenting of the large track lengths to be encountered.

REFERENCE

- 1) "Sweepnik Performance to Date", O.R. Frisch and G.S.B. Street, Proc. of a Seminar on Future Development of Automatic Bubble Chamber Film Measurement held at the Rutherford Laboratory; RHEL/R183 p. 10, October 1968.

Figures

1. Helix fit error derived from 16 Gev/c $pp \rightarrow pp\pi^+\pi^-$ events.
- 2a. A 3-prong event with closed-circuit TV reference cross centred on vertex.
- 2b. Analogue signal and squared pulses obtained when reference cross is positioned on 3-prong event as in Figure 2a.
3. Helix fit error derived from 4800 tracks of 3-prongs from 8 Gev/c np collisions.
- 4a. χ^2 distribution and 4b. probability distribution, from fitted events of the type $np \rightarrow pp\pi^-$
5. Missing-mass distribution from fitted events of the type $np \rightarrow pp\pi^-$.
6. θ/s plots: (i.) a 16 Gev/c proton track with only random fluctuations about a constant $d\theta/ds$; (ii) a low momentum track with large ionization loss; (iii) probe has derailed onto the wrong track.
7. θ/s plot from a bremsstrahlung in which the electron has lost 53% of its energy.
8. Experimental error distribution in θ when the RMS angle error has been taken as 1.3 counts: the quantity plotted is $(\chi^2 - f) / \sqrt{2f}$, where f is the number of degrees of freedom ($= n-1$, where n is the number of points measured on the track).
9. Analogue signals from two closely spaced tracks in the BEBC model chamber
a. before filtering, and b. after filtering.

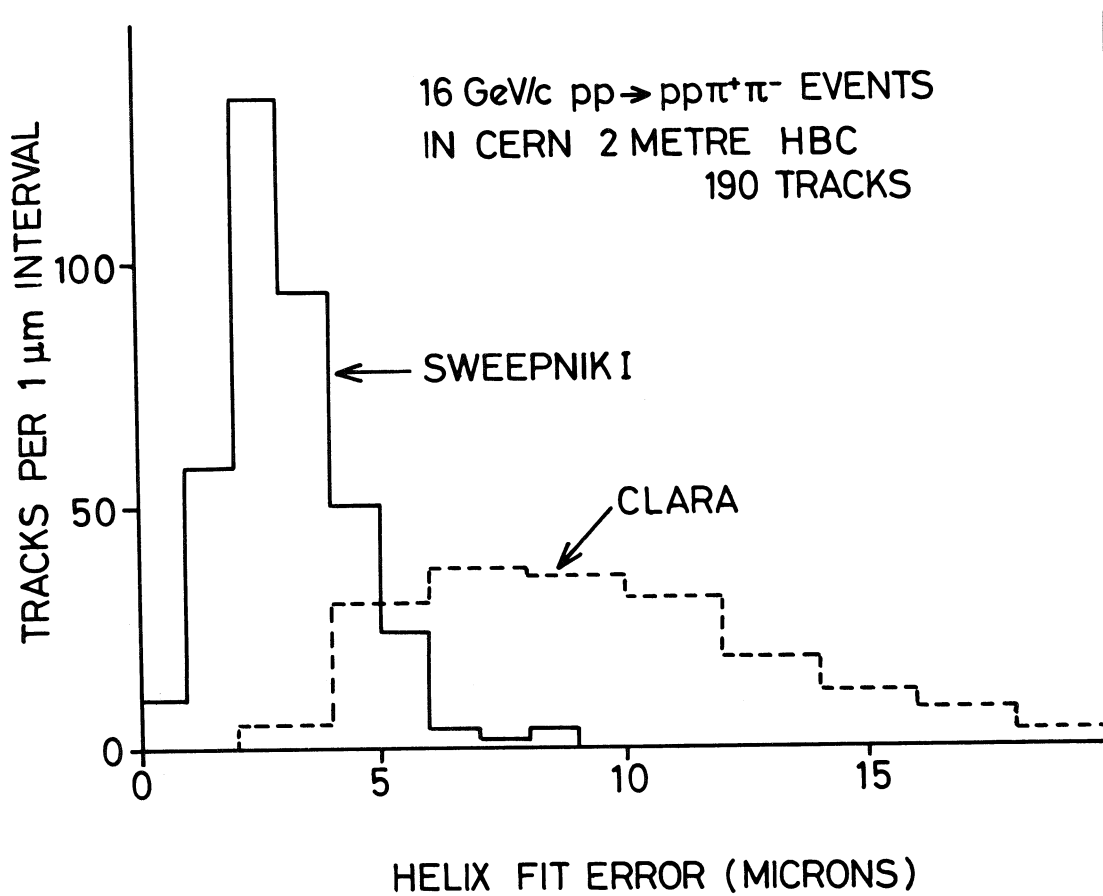


Fig. 1

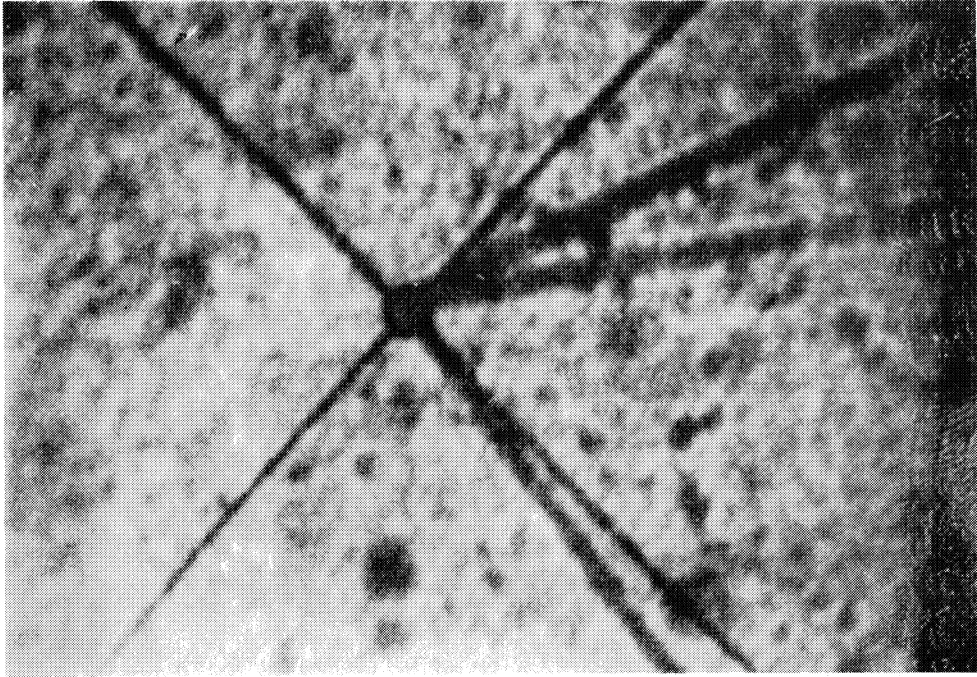


Fig. 2a

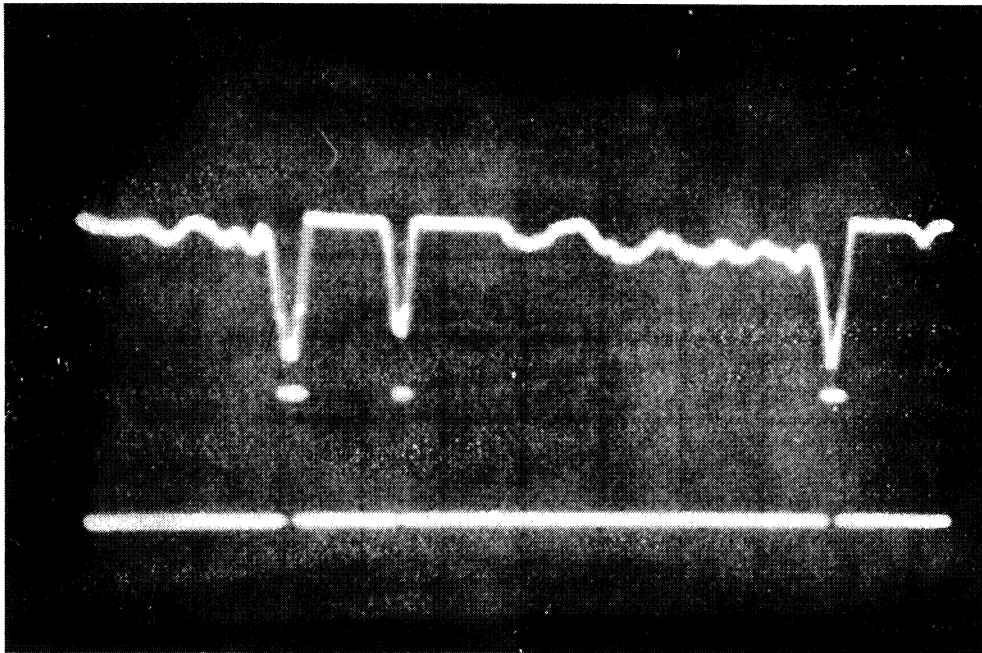


Fig. 2b

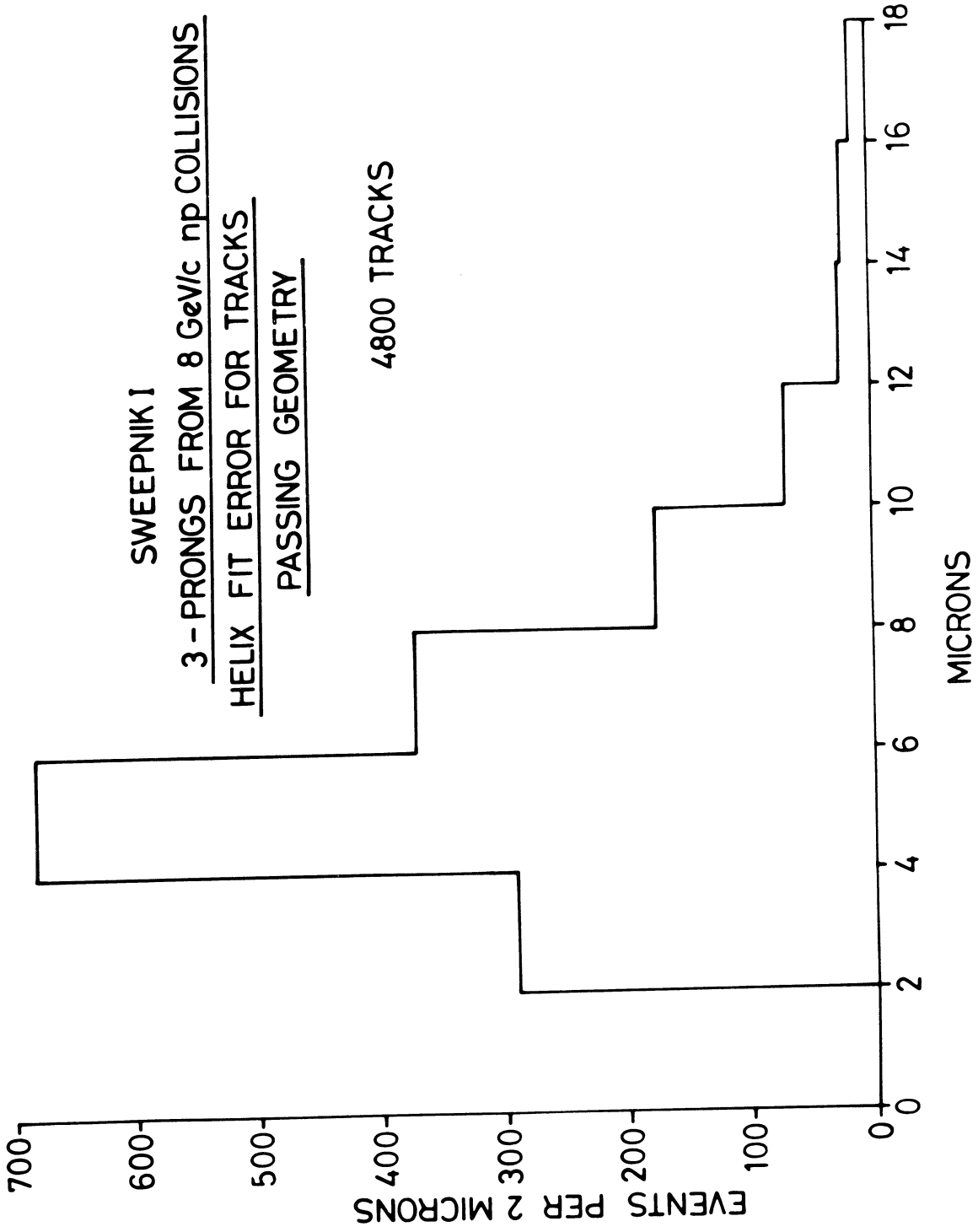


Fig. 3

SWEEPNIK I
CHI-SQUARED HISTOGRAM FOR PPT⁻ EVENTS

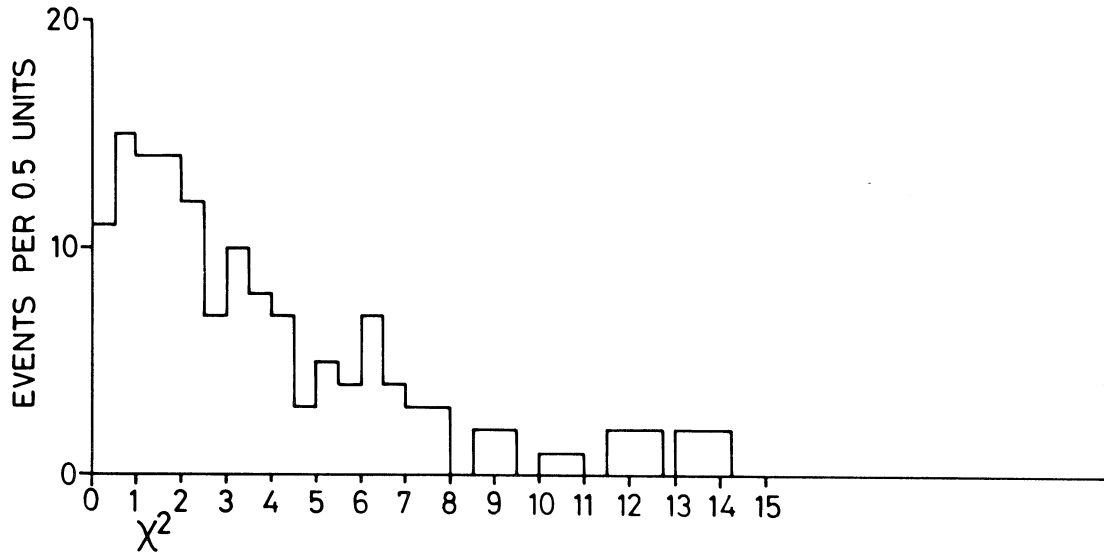


Fig. 4a

SWEEPNIK I
CHI-SQUARED PROBABILITY FOR FITTED PPT⁻

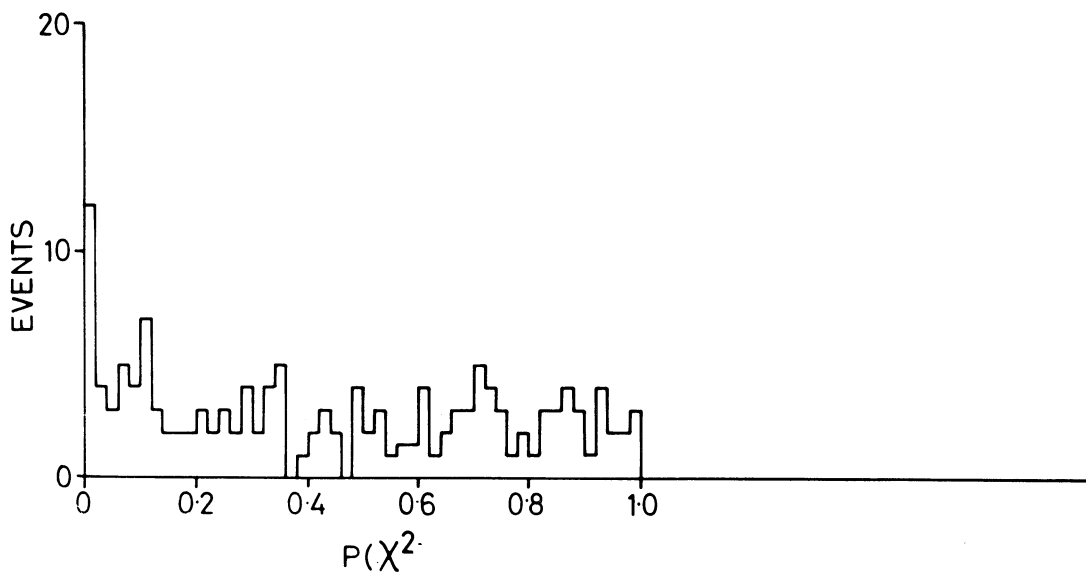


Fig. 4b

SWEEPNIK I
MISSING MASS HISTOGRAM FOR EVENTS
FITTING AS PPT $\bar{\nu}$

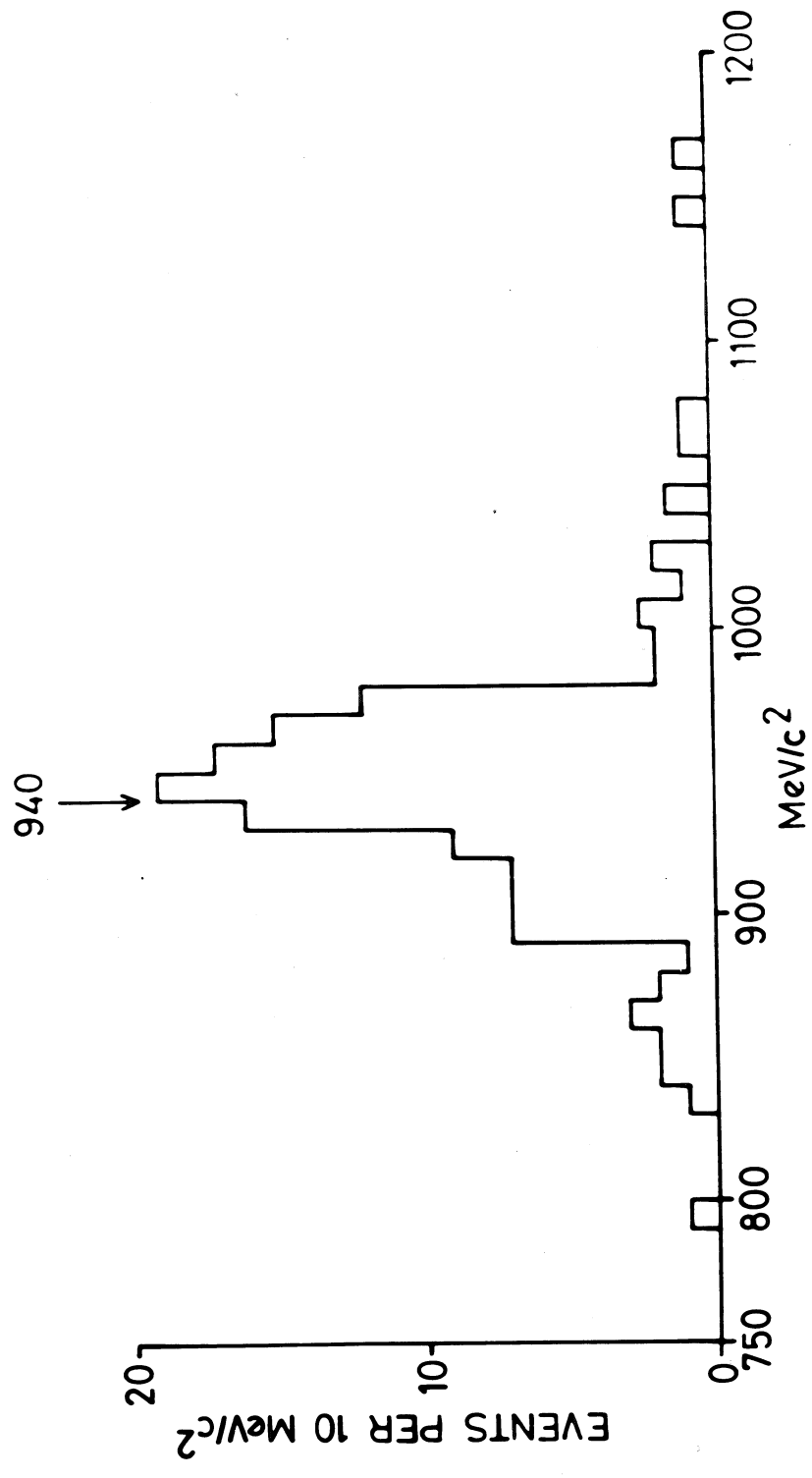


Fig. 5

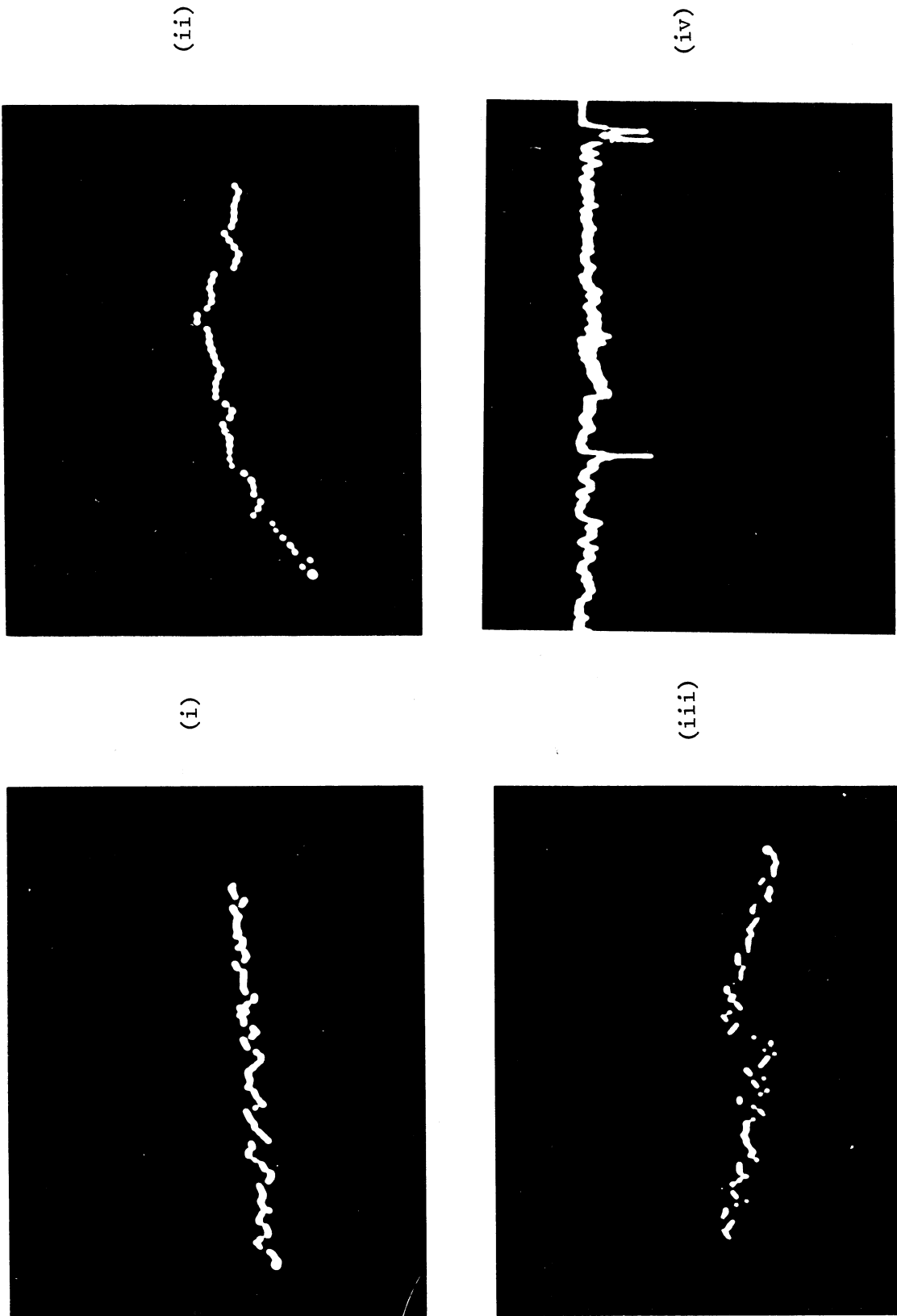


Fig. 6

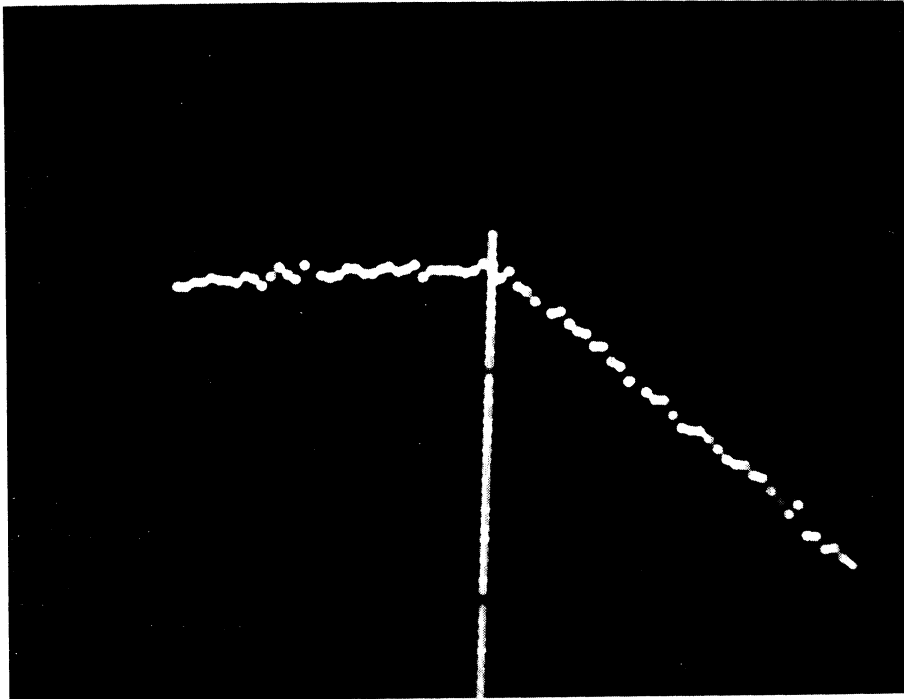


Fig. 7

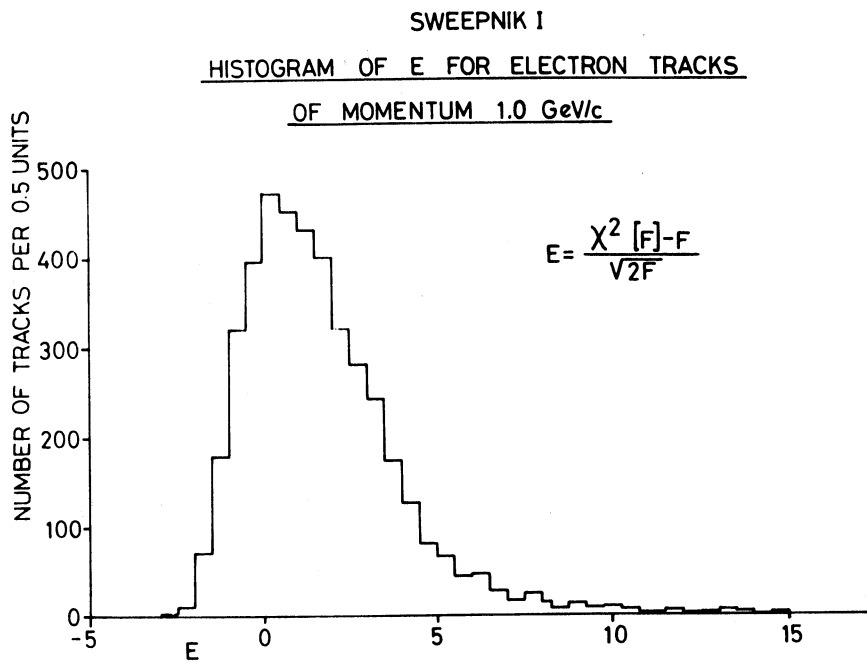


Fig. 8

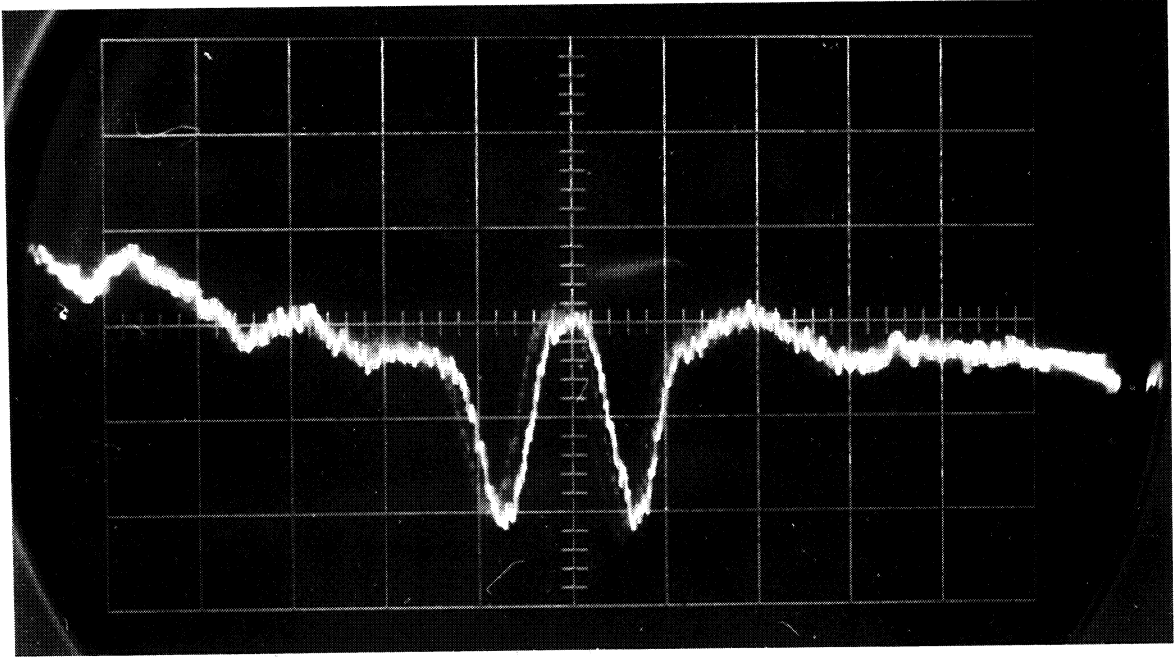


Fig. 9a

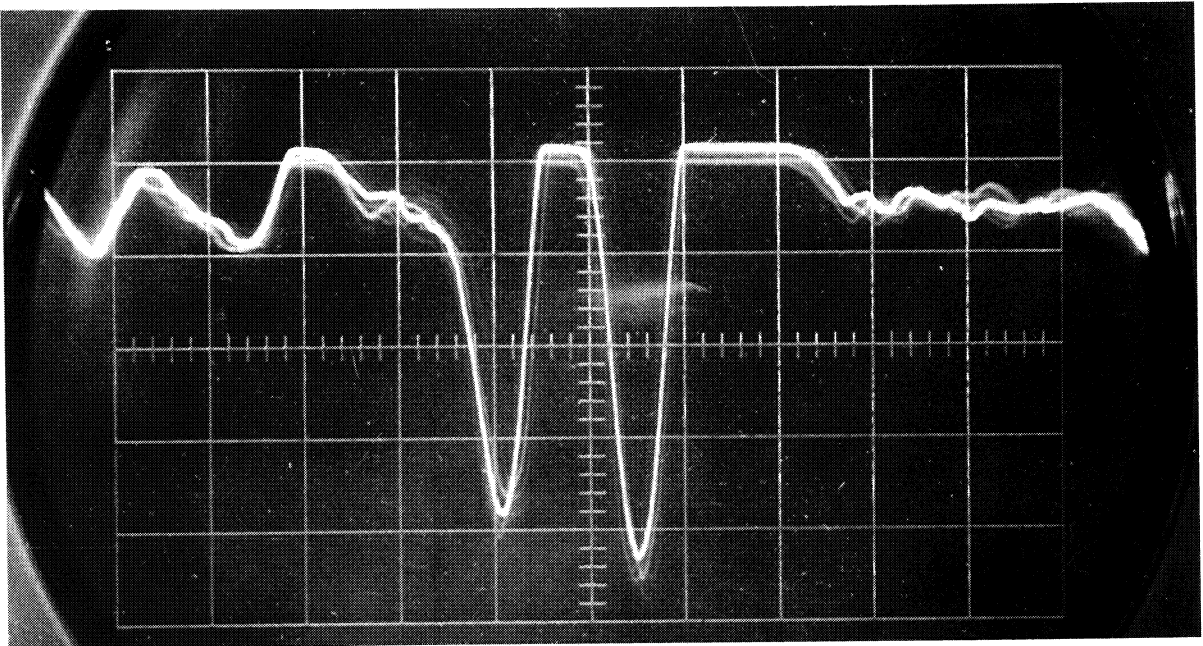


Fig. 9b

DISCUSSION

A. WERBROUCK (*Torino*): What is the angular width of the gate on the sweep?

G. STREET: It's variable. We usually use a 5° gate, when track following, but we start off with quite a wide gate, until the track is established.

R. ROYSTON (*SCS*): How close can tracks get before they become confused?

G. STREET: This is given by the line width*, so approximately one track width is needed between the edges of the two tracks. If they are nearer than this at the moment, we are in trouble.

P.J. DORNAN (*Imperial College*): Does Sweepnik attempt to determine ionization?

G. STREET: Some hardware has been thought about for doing a separate point scan along the track but first we will investigate the information we already have, which is the discrimination level (this is set by the computer) and the pulse width.

P.J. DORNAN (*Imperial College*): You do not look at pulse height?

G. STREET: Not yet, we shall do so before we embark on new hardware.

* In Professor Frisch's talk this was stated to be about $50 \mu\text{m}$ for Sweepnik I and about $15 \mu\text{m}$ for Sweepnik II.